Journal of Power Sources 203 (2012) 72–77

Contents lists available at SciVerse ScienceDirect

Journal of Power Sources

journal homepage: www.elsevier.com/locate/jpowsour

Co_3O_4 as anode material for thin film micro-batteries prepared by remote plasma atomic layer deposition

M.E. Donders[a,b], H.C.M. Knoops[a,b], W.M.M. Kessels[b], P.H.L. Notten[b,*]

[a] Materials innovation institute M2i, P.O. Box 5008, 2600 GA Delft, Netherlands
[b] Eindhoven University of Technology, P.O. Box 513, 5600 MB Eindhoven, Netherlands

ARTICLE INFO

Article history:
Received 7 July 2011
Received in revised form
29 November 2011
Accepted 9 December 2011
Available online 17 December 2011

Keywords:
Cobalt oxide
Atomic layer deposition
Lithium-ion
Battery
Anode

ABSTRACT

Cobalt oxide thin films have been deposited with remote plasma atomic layer deposition (ALD) within a wide temperature window (100–400 °C), using $CoCp_2$ as cobalt precursor and with a remote O_2 plasma as oxidant source. The growth rate was relatively high at 0.05 nm per ALD-cycle and resulted in the deposition of high density (~5.8 g cm^{-3}), stoichiometric Co_3O_4. For the electrochemical analyses, Co_3O_4 was deposited on a Si substrate covered with an ALD-synthesized TiN layer to prevent Li diffusion. The as-deposited electrodes were investigated in a three-electrode electrochemical cell using constant current (CC) charge/discharge cycling and Galvanostatic Intermittent Titration Technique (GITT) in combination with Electrochemical Impedance Spectroscopy (EIS). Compared to the literature, ALD-deposited Co_3O_4 exhibited a high electrochemical activity (~1000 mAh g^{-1}) and the formation of a solid electrolyte interface has been identified by EIS.

1. Introduction

Negative electrode materials remain an important topic in the improvement of rechargeable lithium ion batteries. In this field, transition metal oxides have proven to be viable candidates to replace the commercially standard carbon as anode material. Even though so-called conversion materials present obvious drawbacks in comparison to intercalation materials, moving towards thin film technology could help to overcome these challenges. Interesting conversion anodes reported in the literature are Fe_2O_3, RuO_2, SnO_2 and Co_3O_4 [1–4].

Co_3O_4 is particularly interesting because compared to commonly used graphite anodes, which have a theoretical capacity of 374 mAh g^{-1}, Co_3O_4 provides a much higher theoretical capacity of 890 mAh g^{-1} while maintaining a good cycle life [5,6]. However Co_3O_4 is a conversion material and it is well known that this type of materials display high overpotentials [4]. In addition, Co_3O_4 anodes show poorer charge transfer kinetics than intercalation anodes due to the formation of Li_2O [6], which generally limits the use of these materials to low power applications.

Thin film all-solid-state devices employ sub-micron layer thicknesses (anode thickness is of the order of 10–100 nm) and this will improve the charge transfer kinetics in this case due to shorter diffusion lengths for lithium ions and less resistance for the electrons. The thin film applications are therefore expected to be able to exploit the benefits of Co_3O_4 anodes. A possible thin film application of these conversion materials is in innovative concepts like the 3D thin film all-solid-state lithium-ion battery as proposed by Notten et al. [5,7].

To effectively integrate this technology in all-solid-state battery applications, it is essential to produce high quality thin films. However, when applying thin films in batteries the capacity of the battery will decrease per footprint area in comparison to conventional bulk materials. To overcome this decrease in storage capacity the film can be made thicker or the surface area can be increased. Increasing the layer thickness would create additional problems related to diffusion and would increase the impedance of the battery stack. Therefore, moving towards 3D battery structures is an elegant way to increase the storage capacity without increasing the layer thickness or increasing the size of the battery [7]. For this reason, step-conformal thin-film deposition techniques, like atomic layer deposition (ALD), are gaining increasingly more interest.

ALD is a surface-chemistry controlled, thin-film, deposition technique with an excellent conformality and thickness control at the atomic scale, even in challenging high aspect ratio structures. In our previous study a Co_3O_4 ALD process has been developed using bis(η^5-cyclopentadienyl)Co(II) ($CoCp_2$) and an O_2 plasma [8]. This deposition technique enables a temperature-independent growth rate for Co_3O_4 of 0.05 nm per ALD-cycle for temperatures

* Corresponding author. Tel.: +31 040 247 30 69; fax: +31 040 245 50 54.
E-mail address: P.H.L.Notten@tue.nl (P.H.L. Notten).

0378-7753/$ – see front matter © 2011 Elsevier B.V. All rights reserved.
doi:10.1016/j.jpowsour.2011.12.020

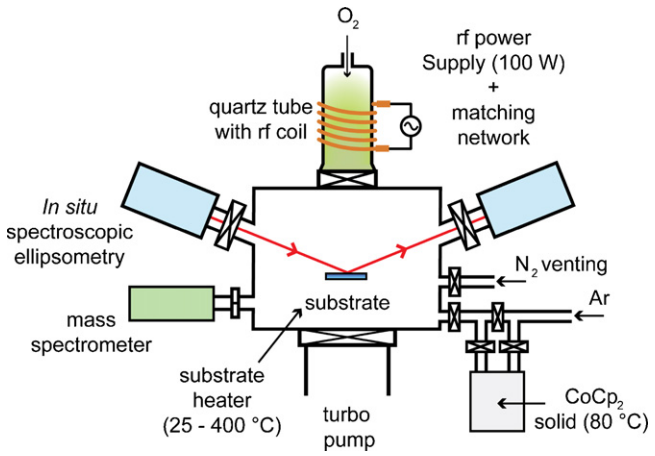

Fig. 1. A schematic overview of the ALD-I setup. Also the *in situ* spectroscopic ellipsometer and mass spectrometer are depicted.

between 100 and 400 °C (measured by *in situ* spectroscopic ellipsometry). A polycrystalline, stoichiometric, Co_3O_4 thin-film was obtained with an average mass density of ~5.8 g cm^{-3}. In addition, this process provides an interesting first step towards the development of ALD-deposited $LiCoO_2$, which is a widely used cathode material.

In literature opinions about the actual reactions taking place in the Co_3O_4 electrode are divided between: (1) a fully reversible reaction of Co_3O_4 [4,6] and (2) an initiation reaction between Co_3O_4 and lithium followed by a reversible reaction employing CoO [5]:

$$Co_3O_4 + 8Li^+ + 8e^- \rightleftarrows 3Co + 4Li_2O \quad (1)$$

$$\begin{cases} Co_3O_4 + 8Li^+ + 8e^- \rightarrow 3Co + 4Li_2O \\ 3Co + 3Li_2O \rightleftarrows 3CoO + 6Li^+ + 6e^- \end{cases} \quad (2)$$

This paper will briefly present the ALD deposition process of Co_3O_4 and a more in depth electrochemical investigation of ALD-synthesized Co_3O_4 as thin film negative electrode using conventional organic liquid electrolyte. In addition the electrochemical results are evaluated to attempt to identify the correct reaction mechanism.

2. Experimental details

2.1. ALD processes

The Co_3O_4 films were deposited using a home-built open-load ALD setup ("ALD-I") as shown schematically in Fig. 1 and as described extensively by Langereis et al. [9]. In this setup an inductively coupled plasma (ICP) source is connected to a deposition chamber along with a pump unit through gate valves. The pump unit consists of a rotary and turbo molecular pump, which can reach a base pressure of <10^{-5} mbar by overnight pumping. The $CoCp_2$ precursor (98%, Strem Chemicals) was heated to 80 °C and bubbled with Ar at a pressure of 0.02 mbar. The substrate was heated to 300 °C, while the reactor walls, Ar lines, and $CoCp_2$ precursor lines were maintained at a temperature of 105 °C. For electrochemical analysis, Co_3O_4 was deposited on a Si substrate covered with a 40 nm ALD-synthesized TiN layer which acts as a current collector and as a barrier layer to prevent the diffusion of lithium into the Si substrate (Fig. 2) [10]. These TiN thin films were deposited using the Oxford Instruments FlexAL reactor, as described by Knoops et al. [10] with $TiCl_4$ as titanium precursor in combination with an H_2–N_2 plasma. Si(1 0 0) (2–3 Ω cm) with native oxide and Si(1 0 0) with 400 nm thermally grown SiO_2 were used as substrates.

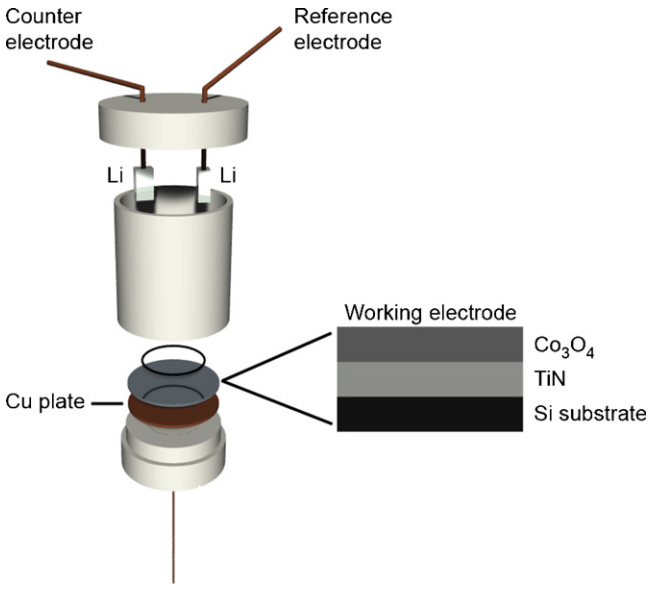

Fig. 2. Schematic representation of the Teflon® three-electrode measurement setup and the working electrode used in the electrochemical measurements.

The first ALD half-cycle of the Co_3O_4 process consists of a 2 s $CoCp_2$ precursor dosing with Ar bubbling. During and after the precursor dosing the reaction products are pumped out. The second half-cycle consists of an O_2 exposure at 0.01 mbar chamber pressure while applying a 100 W plasma power for 5 s.

2.2. Electrochemical analysis

The electrochemical analyses were performed in three-electrode cylindrical electrochemical cells with an effective measurement surface area of 2 cm^2 (Fig. 2), made of Teflon® with a volume of about 15 ml. The cells were assembled in an argon-filled glove-box. The cobalt oxide electrodes were mounted as the working electrodes while pure lithium foils were used as counter and reference electrodes. 1 molar $LiPF_6$ dissolved in ethyl carbonate (EC)/diethyl carbonate (DEC) was used as liquid electrolyte and was provided by Puriel, Techno, Semichem Co., Ltd., Korea. The cells were placed in a stainless steel holder that was thermostatically controlled at room temperature. Contaminants in the glove-box (water and oxygen) were monitored and controlled below 1 ppm. Galvanostatic cycling was performed with a M2300 galvanostat (Maccor, Tulsa, USA). Galvanostatic Intermittent Titration Technique (GITT) and Electrochemical Impedance Spectroscopy (EIS) were conducted with an Autolab PGSTAT30 (Ecochemie B.V., Utrecht, The Netherlands). The following definitions are adopted throughout the manuscript: discharging an electrode material refers to Li-ion insertion (or lithiation) and charging to Li-ion extraction (or delithiation). 1 C-rate is defined as the current required to (dis)charge the electrode in 1 h (46.4 μA for 1000 mAh g^{-1}).

3. Results and discussion

3.1. ALD process

A remote plasma ALD process for Co_3O_4 has been developed using the combination of $CoCp_2$ as cobalt precursor and O_2 plasma as oxidant source [8]. The temperature window for the Co_3O_4 process was found to be broad, ranging from 100 to 400 °C with an almost temperature-independent growth rate of 0.05 nm per ALD-cycle (Fig. 3). Stoichiometric Co_3O_4 was obtained in the whole

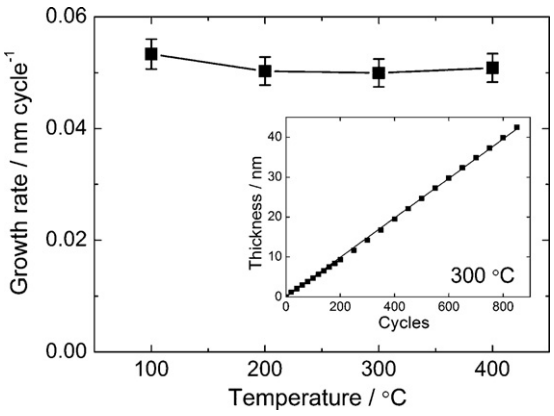

Fig. 3. Growth rate of Co_3O_4 on Si(1 0 0) as a function of the substrate temperature. Inset: linear growth is observed for 300 °C (as well as for the other substrate temperatures investigated).

temperature range investigated and the average mass density measured was 5.8 g cm^{-3} showing no dependence on temperature. The root-mean-square (RMS) roughness, as measured by AFM, was ≤1 nm for all film thicknesses and substrate temperatures investigated and smoother films are obtained than reported in the literature [11].

X-ray diffraction showed cubic Co_3O_4 films with a strong preferential (1 1 1) direction for all substrate temperatures, while a (1 0 0) preferential orientation was reported in the literature at low substrate temperatures and a (1 1 1) orientation at high temperatures [11]. Interestingly, this reveals that the surface roughness and specific orientation are not significantly influenced by conditions such as substrate temperature and film thickness [8]. These differences in these results could be related to either the use of $CoCp_2$ as precursor instead of $Co(thd)_2$ or to the use of a remote O_2 plasma process instead of ozone. Moreover XRD, SE and FTIR independently indicate an increasing crystallinity with substrate temperature, while the surface roughness remains low. Mass spectrometric measurements reveal a combustion-like reaction process with CO, CO_2 and H_2O as reaction by-products [8].

3.2. Electrochemical investigations

To evaluate the use of ALD grown cobalt oxide as anode material in a battery application, samples of 40 nm ALD Co_3O_4 on 40 nm ALD TiN were investigated using constant current (CC) charge/discharge cycling and Galvanostatic Intermittent Titration Technique (GITT) in combination with Electrochemical Impedance Spectroscopy (EIS).

Constant current (CC) charge/discharge cycling of Co_3O_4 was performed with 1 and 5 μA (0.02 and 0.11 C, respectively). Fig. 4 shows that cobalt oxides present a relatively high overpotential which limits the use of these layers to low power applications that require a slow exchange of energy and thus a slow exchange of Li^+ ions between the anode and cathode. However, because these films are in the nanoscale, it is expected that the overpotential of this layer will not induce a large problem in less demanding power applications of such all-solid-state devices.

A series of constant current measurements were carried out with a charge rate varying from ~0.02 C to ~22 C. Before changing the applied current, the electrode was pre-treated with a deep (dis)charge current of 1 μA to ensure a constant base condition. The amount of charge that can be stored and extracted in the electrode with increasing current was found to exhibit a fast decline (Fig. 5A and B), but the sample remained stable throughout the measurements. If a capacity of ~1000 mAh g^{-1} is desired, a

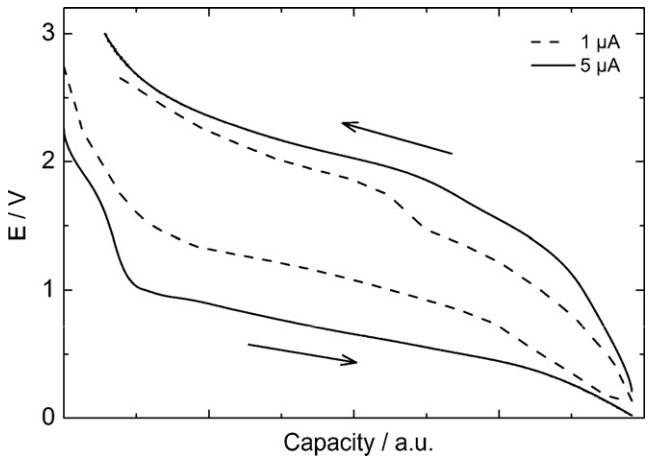

Fig. 4. Constant current (CC) charge/discharge cycling between 20 mV and 3 V (applying 1 and 5 μA, 0.02 and 0.11 C-rate respectively) of ALD Co_3O_4 on TiN/Si using $LiPF_6$ in ethylene carbonate/diethyl carbonate (EC/DEC, 1/1) as liquid electrolyte. The graph displays a large overpotential and an ~7% capacity loss between charge and discharge. The two graphs have been normalized for comparison and therefore the *x*-axis is displayed using arbitrary units (a.u.).

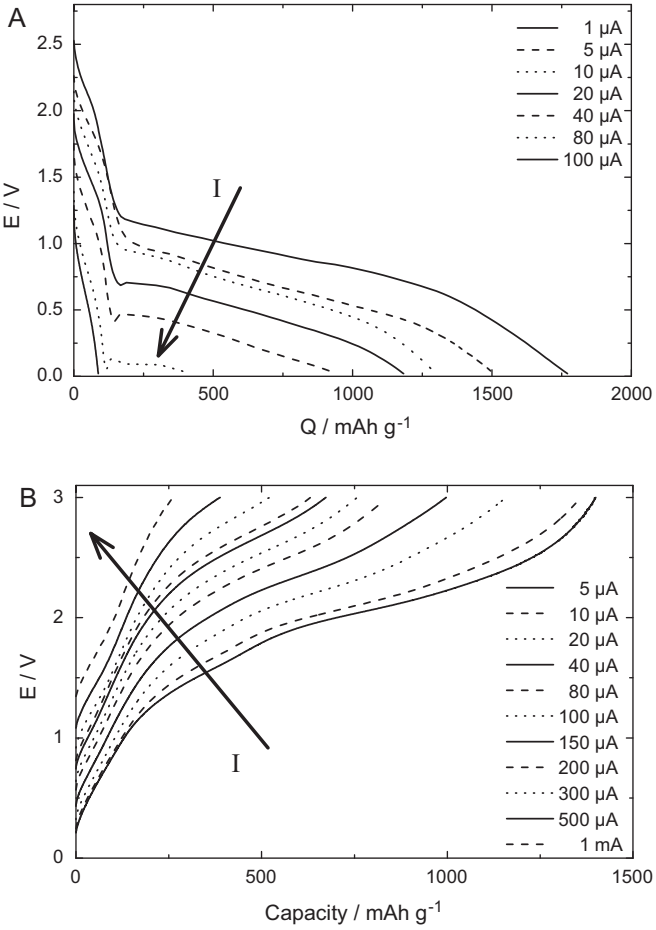

Fig. 5. (A) Discharge curves of a Co_3O_4 electrode as function of gravimetric storage capacity (*Q*) for various currents. 1 C-rate corresponds to 46.4 μA. (B) Charge curves of a Co_3O_4 electrode as function of gravimetric storage capacity for various currents. 1 C-rate corresponds to 46.4 μA.

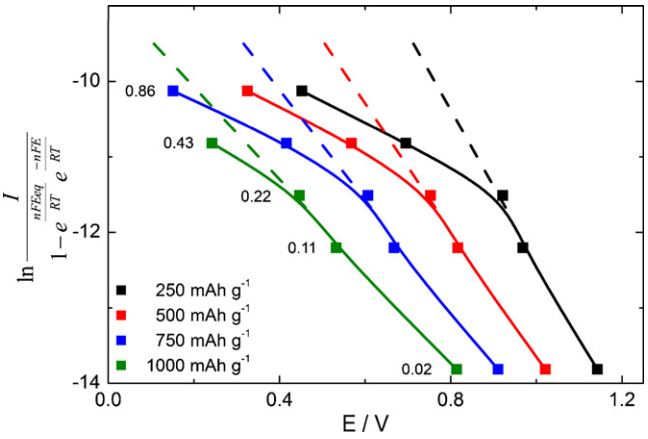

Fig. 6. Butler–Volmer data plotted as a function of the electrode potential at the selected gravimetric storage capacities 250, 500, 750 and 1000 mAh g^{-1} (calculated from Fig. 5A). The numbers in the graph correspond to the applied C-rate.

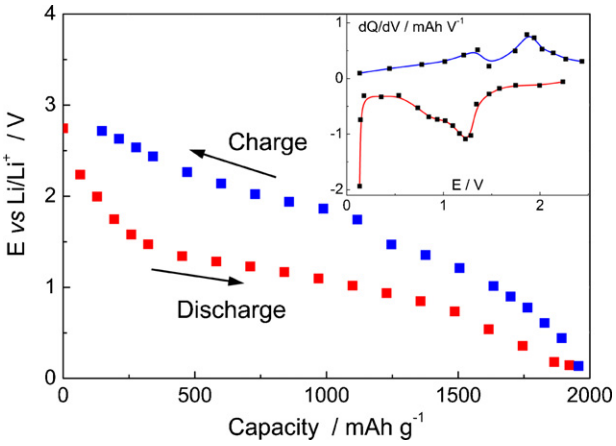

Fig. 7. Equilibrium potential *versus* the discharge capacity of Co_3O_4 during GITT. The A-C references indicate to the corresponding part in Fig. 8 for the specific voltage range and the inset displays the position of the sloping plateau in the main graph.

maximum applied charge current of ~40 μA (~0.86 C-rate) can be used to extract all the Li from the Co_3O_4 negative electrode. However, during discharge it was not possible to apply a current much higher than 1 C-rate to the electrode due to the very rapid decrease in storage capacity as can be seen in Fig. 5A. This means that it will take a longer time to load a stack employing Co_3O_4 as anode with lithium ions than to extract.

The Butler–Volmer equation (Eq. (3)) has been used in order to quantify the charge transfer kinetics of Co_3O_4 thin-film electrodes in more detail:

$$I = I_0(e^{(\alpha nF\eta)/(RT)} - e^{(-(1-\alpha)nF\eta)/RT}) \quad (3)$$

in which I_0 is the exchange current density (A cm^{-2}), α the symmetry factor of the charge transfer reaction, F the Faraday constant (96,485 C mol^{-1}), η the overpotential, defined as the difference between the potential under current flowing conditions (E) and the equilibrium potential (E_{eq}), R the gas constant (8.314 J mol^{-1} K^{-1}) and T is the absolute temperature [12]. Transforming this equation leads to a logarithmic form:

$$\ln \frac{I}{1 - e^{(-nFE_{eq})/(RT)}e^{(nFE)/(RT)}} = \ln I_0 + \frac{\alpha nFE_{eq}}{RT} - \frac{\alpha nFE}{RT} \quad (4)$$

The left-hand side of Eq. (4) is a linear function of the measured electrode potential (E) and the experimental results obtained at four different storage capacities (250, 500, 750 and 1000 mAh g^{-1}) are presented in Fig. 6. The data reveals a clear linear dependence up to discharge currents of 0.22 C-rate (10 μA), indicating that the charge transfer reaction at the electrode/electrolyte interface is the rate-determining step. From the slope of these curves α can be extracted while the intercept provides information about the exchange current densities at the various stages of the conversion process. At higher discharge currents deviation from linearity starts to occur, which is attributed to mass-transport limitations inside the thin film [12].

The GITT analysis was performed with 20 incremental discharge steps at 1 μA of either 3 or 6 h, with resting periods of 3 h in between the steps. The end of a resting period can be considered as equilibrium and at this point EIS is performed in a frequency range of 1 MHz to 0.5 Hz. Fig. 7 displays the equilibrium voltage *versus* the storage capacity and a sloping plateau is visible between 1.3 and 0.8 V. This is made more clear by the dQ/dE *versus* $E(V)$ graph shown in the inset of Fig. 7, where the peak corresponds to the position of the plateau. This position is in agreement with the broad cathodic current peak found in cyclic voltammetric measurements performed by Yao et al. [13] and corresponds to the phase transition of cobalt oxide to Co metal and Li_2O.

At each point in the equilibrium graph of Fig. 7 an impedance measurement is performed. The results are presented in three groups in Fig. 8. For relatively high equilibrium voltages the impedance profiles are displayed in Fig. 8A where a second semi-circle appears around 2 V, indicating the formation of a solid electrolyte interface (SEI), similar as found for conventional graphite electrodes. Fig. 8B and C represent the impedance profiles at the first and the second half of the sloping plateau, respectively, and show that the impedance of the electrode increases at lower voltages when more and more Li^+ ions react with Co_3O_4 to form Co metal and Li_2O. By equivalent circuit fitting, the resistance and capacitance of the SEI layer are obtained for the measured voltage range. The results are plotted in Fig. 8D and clearly shows that the resistance of the SEI layer increases significantly between 1.3 and 0.8 V where the phase transition to Co metal and Li_2O takes place. These results show that using GITT analyses, revealing the equilibrium voltage curve, in combination with EIS can be used to characterize both the thermodynamics and the kinetics of ALD deposited Co_3O_4 electrodes during electrochemical charging and discharging.

When applying Co_3O_4 in all-solid-state batteries the layer will be covered by a solid-state electrolyte as *e.g.* LiPON. In this case the decomposition of the liquid electrolyte would be prevented and the formation of a SEI layer would be completely absent, as shown by Baggetto et al. for Si negative electrodes [12,13]. This effect can extend the lifetime of the battery significantly.

The lifetime of the electrode was evaluated using constant current charge/discharge cycling applying a current of 10 μA (0.22 C) and the capacity initially decreased during the first 15 cycles (Fig. 9). After this decrease however, the capacity is stabilized and even increased to ~1000 mAh g^{-1} after 70 cycles. This phenomenon was also observed by Pralong et al. for layers deposited with pulsed laser deposition (PLD) and has been attributed to the occurrence of a second redox process involving the electrolyte [4]. The capacity after 20–70 cycles shows a drop of 20–30% when comparing to the first cycle capacity. Comparing these results with the two different reaction mechanisms suggested in literature, this capacity drop would suggest in favor of an irreversible reaction from Co_3O_4 to Li_2O and Co followed by the reversible cycling of CoO (Eq. (2)). Theoretically this first irreversible step is accompanied by the loss of 25% capacity compared to fully reversible Co_3O_4 and correlates well with our experimental values.

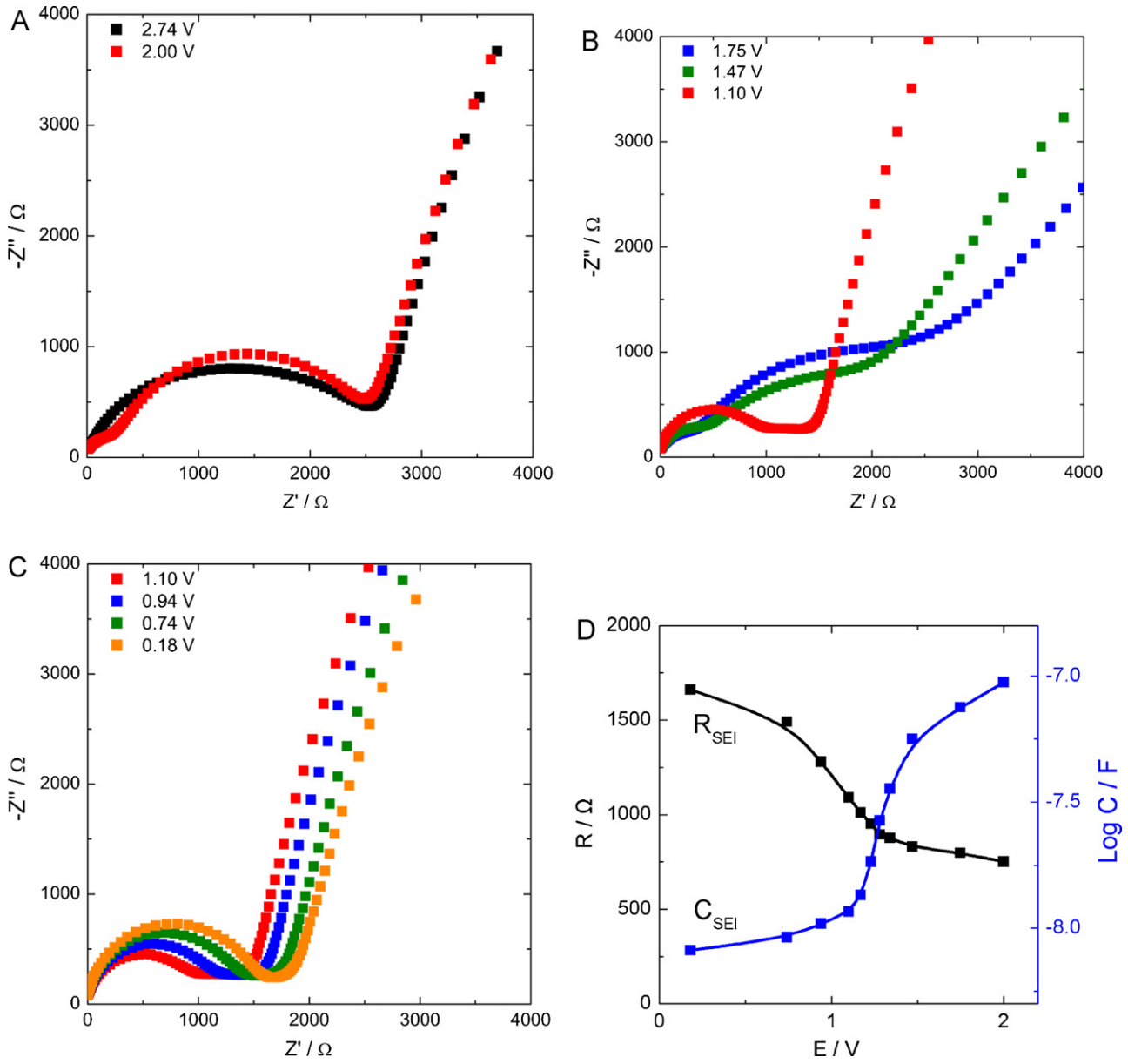

Fig. 8. Impedance spectra during GITT analysis at potentials of (A) above 2 V, (B) between 1 and 2 V and (C) between 0 and 1 V *versus* Li/Li^+. The parameters of an equivalent circuit were determined and plotted in D.

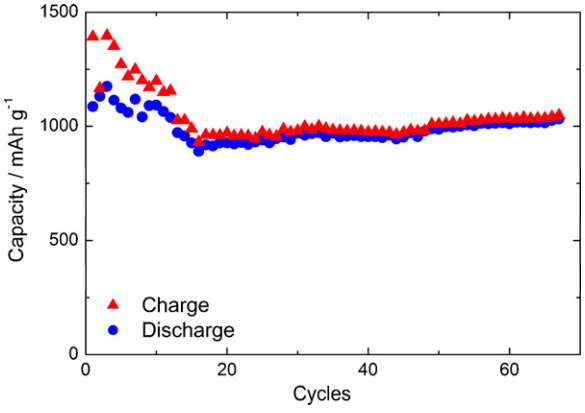

Fig. 9. Capacity of a Co_3O_4 electrode *versus* cycle number. The electrode was cycled between 20 mV and 3 V at 10 μA (0.22 C) with a half hour resting period in between the cycles, using using $LiPF_6$ in ethylene carbonate/diethyl carbonate (EC/DEC, 1/1) as liquid electrolyte.

4. Conclusions

A remote plasma ALD process for Co_3O_4 was developed using the combination of $CoCp_2$ as cobalt precursor and O_2 plasma as oxidant source. The temperature window for the Co_3O_4 was found to be broad, ranging from 100 to 400 °C with a virtually temperature independent growth rate of 0.05 nm per ALD-cycle.

The charge/discharge capacity initially decreased during the first 15 cycles to stabilize afterwards and even increased to ~1000 mAh g^{-1} after 70 cycles. When compared to a capacity of 374 mAh g^{-1} for graphite negative electrodes this is a very competitive capacity and the weight of the anode can almost be reduced by three for the same battery capacity. In addition a thinner film will decrease the diffusion path length for lithium in the Co_3O_4 layer and can help with overcoming the high overpotential presented by this material. The thin film application is therefore expected to be able to exploit the benefits of Co_3O_4 anodes.

Further, it is shown that using a GITT analysis in combination with EIS can be used to investigate the impedance behavior of the ALD Co_3O_4 electrode and SEI formation during the loading with lithium.

Acknowledgement

This work was sponsored by the Materials innovation institute M2i under project number MC3.06278.

References

[1] H. Liu, G. Wang, J. Park, J. Wang, H. Liu, C. Zhang, Electrochim. Acta 54 (2009) 1733.
[2] P. Balaya, H. Li, L. Kienle, J. Maier, Adv. Funct. Mater. 13 (2003) 621.
[3] Y.-J. Kim, H. Lee, H.-J. Sohn, Electrochem. Commun. 11 (2009) 2125.
[4] V. Pralong, J.-B. Leriche, B. Beaudoin, E. Naudin, M. Morcrette, J.-M. Tarascon, Solid State Ionics 166 (2004) 295.
[5] H.-C. Liu, S.-K. Yen, J. Power sources 166 (2007) 478.
[6] Y.-M. Kang, M.-S. Song, J.-H. Kim, H.-S. Kim, M.-S. Park, J.-Y. Lee, H.K. Liu, S.X. Dou, Electrochim. Acta 50 (2005) 3667.
[7] P.H.L. Notten, F. Roozeboom, R.A.H. Niessen, L. Baggetto, Adv. Mater. 19 (2007) 4564.
[8] M.E. Donders, H.C.M. Knoops, M.C.M. van de Sanden, W.M.M. Kessels, P.H.L. Notten, J. Electrochem. Soc. 158 (2011) G92.
[9] E. Langereis, H.C.M. Knoops, A.J.M. Mackus, F. Roozeboom, M.C.M. van de Sanden, W.M.M. Kessels, J. Appl. Phys. 102 (2007) 083517.
[10] H.C.M. Knoops, L. Baggetto, E. Langereis, M.C.M. van de Sanden, J.H. Klootwijk, F. Roozeboom, R.A.H. Niessen, P.H.L. Notten, W.M.M. Kessels, J. Electrochem. Soc. 155 (2008) G287.
[11] K.B. Klepper, O. Nilsen, H. Fjellvåg, Thin Solid Films 515 (2007) 7772.
[12] L. Baggetto, R.A.H. Niessen, F. Roozeboom, P.H.L. Notten, Adv. Funct. Mater. 18 (2008) 1057.
[13] W. Yao, J. Yang, J. Wang, Y. Nuli, J. Electrochem. Soc. 155 (2008) A903.